Atmos. Chem. Phys. Discuss., doi:10.5194/acp-2017-258, 2017
Manuscript under review for journal Atmos. Chem. Phys.
Discussion started: 10 April 2017

Atmospheric Chemistry and Physics Discussions

Seasonal characteristics, formation mechanisms and geographical origins of $PM_{2.5}$ in two megacities in Sichuan Basin, China

Huanbo Wang[1,2], Mi Tian[1], Yang Chen[1], Guangming Shi[1], Yuan Liu[1], Fumo Yang[1,2,3,4*], Leiming Zhang[5], Liqun Deng[6], Jiayan Yu[7], Chao Peng[1], and Xuyao Cao[1]

[1]Research Center for Atmospheric Environment, Chongqing Institute of Green and Intelligent Technology, Chinese Academy of Sciences, Chongqing, 400714, China

[2]Chongqing University, Chongqing, 400044, China

[3]Center for Excellence in Regional Atmospheric Environment, Institute of Urban Environment, Chinese Academy of Sciences, Xiamen, 361021, China

[4]Yangtze Normal University, Chongqing, 408100, China

[5]Environment and Climate Change Canada, Toronto, Canada

[6]Sichuan Academy of Environmental Sciences, Chengdu, 610041, China

[7]Chongqing Environmental Monitoring Center, Chongqing 401147, China

Correspondence to: Fumo Yang (fmyang@cigit.ac.cn)

Atmos. Chem. Phys. Discuss., doi:10.5194/acp-2017-258, 2017
Manuscript under review for journal Atmos. Chem. Phys.
Discussion started: 10 April 2017

Atmospheric Chemistry and Physics Discussions

Abstract. To investigate the characteristics of $PM_{2.5}$ and its major chemical components, formation mechanisms, and geographical origins in the two biggest cities, Chengdu (CD) and Chongqing (CQ) in Sichuan Basin, the most densely populated basin in China, daily $PM_{2.5}$ samples were collected simultaneously at one urban site in each city from October 2014 to July 2015. Annual mean concentrations of $PM_{2.5}$ were 67.0 ± 43.4 and 70.9 ± 41.4 μg m^{-3} at CD and CQ, respectively. Secondary inorganic aerosols (SNA) and organic matter (OM) accounted for 41.1% and 26.1%, respectively, of $PM_{2.5}$ mass at CD, and 37.4% and 29.6% at CQ. Seasonal variations of $PM_{2.5}$ and its major chemical components were significant, usually with the highest values in winter and the lowest in summer. SNA and OM were 1.7-3.4 times higher on polluted days than on clean days at both sites, whereas their percentage contributions to $PM_{2.5}$ varied differently among the components and between the two sites. Gas-phase oxidation probably played an important role on the formation of secondary aerosols when $PM_{2.5}$ mass varied in the range of 75-150 μg m^{-3}, while heterogeneous transformation was likely the major mechanism on the heavy polluted days. Geographical regions causing high $PM_{2.5}$ were identified to mainly distribute within the basin at both sites based on potential source contribution function (PSCF) analysis.

Atmos. Chem. Phys. Discuss., doi:10.5194/acp-2017-258, 2017
Manuscript under review for journal Atmos. Chem. Phys.
Discussion started: 10 April 2017

Atmospheric Chemistry and Physics Discussions

1 Introduction

Fine particles ($PM_{2.5}$, particulate matter with an aerodynamic diameter smaller than 2.5 μm) have adverse effects on human health (Anderson et al., 2012; Lepeule et al., 2012; Taus et al., 2008), deteriorate air quality (Zhang et al., 2008; Paraskevopoulou et al., 2015), reduce atmospheric visibility (Fu et al., 2016; Cao et al., 2012; Baumer et al., 2008), impact climate (Ramanathan and Feng, 2009; Hitzenberger et al., 1999; Mahowald, 2011), and affect ecosystem (Larssen et al., 2006). In the past two decades, China has experienced serious $PM_{2.5}$ pollution due to the rapidily incresing energy consumption through econmic development, industrialization and urbanization (Tie and Cao, 2009). The National Ambient Air Quality Standards (NAAQS) for $PM_{2.5}$ was promulgated by the Chinese government in 2012, and strict strategies have been implemented nationwide, e.g. controling SO_2 emissions by installing desulphurization system in coal-fired power plants and conversion of fuel to natural gas (Lu et al., 2011), mitigating NO_x emissions through traffic restrictions, and reducing biomass burning through straw shredding. Despite these efforts, there are still many cities that have not met the current NAAQS. According to the '2013-2015 Reports on the State of Environment of China', annual mean concentration of $PM_{2.5}$ in all the74 major cities over China was 72, 64, and 50 μg m^{-3} in 2013, 2014 and 2015, respectively, and only 4.1%, 12.2% and 22.5% of the monitored cities met the NAAQS (35 μg m^{-3}).

Previous studies showed that Beijing-Tianjin-Hebei area (BTH), Yangtze River Delta (YRD), Pearl River Delta (PRD), and Sichuan Basin were the four main regions in China with severe aerosol pollution. While many studies have been conducted in BTH, PRD and YRD regions to understand the general characteristics of $PM_{2.5}$ and its chemical components, formation mechanism, and sources (Ji et al., 2016; Li et al., 2015; Quan et al., 2015; Tan et al., 2016; Yang et al., 2015; Zhang et al., 2013; Zhao et al., 2015; Zhao et al., 2013a; Cheng et al., 2015; Zheng et al., 2015a; Yang et al., 2011a), only a few studies have focused on Sichuan Basin (Tao et al., 2014; Tian et al., 2013; Yang et al., 2011b). Covering an area of 260,000 km^2 with a population of around 100 million in southwest China, the Sichuan Basin is a subtropical expanse of low hills and plains and the most populated basin in China. It is completely encircled by high mountains, and characterized by persistently high relative humidity, and extremely low wind speeds all the year-round (Mengting et al., 2016; Chen and Xie, 2013). It is supposed that the characteristics of $PM_{2.5}$ in Sichuan Basin should be very different from those in eastern coastal China (i.e. PRD and YRD) and North China Plain (i.e. BTH) due to its special

topography and meteorological conditions, besides emission sources. More specifically, the terrain of the two megacities in the basin are distinct from each other, i.e., Chongqing is a mountainous municipality lying on the eastern margin of the basin while Chengdu is located in a completely flat west. Therefore, there is a great interest in comparing the chemical components of $PM_{2.5}$ and characterizing pollution episodes between Chengdu and Chongqing.

The present study aims to fill this gap by measuring chemically-resolved $PM_{2.5}$ in Chengdu and Chongqing in four seasons during 2014-2015. The main objectives are to: (1) characterize the seasonal and site differences of $PM_{2.5}$ and its major chemical components at the two urban sites in Sichuan Basin; (2) compare the $PM_{2.5}$ chemical components under different $PM_{2.5}$ levels and identify the major chemical components that are responsible for $PM_{2.5}$ pollution episodes; (3) explore the possible formation mechanism of the secondary organic and inorganic aerosols; and (4) reveal the geographical regions causing high $PM_{2.5}$ levels through potential source contribution function (PSCF) analysis. The comparison of the differences of $PM_{2.5}$ in this paper provides insight regarding the extent to which fine particulate pollution can vary in terms of in chemical composition, formation mechanisims, and geographical origins between the two megacities in a great basin. This information has implications for better understanding the reasons for heavy haze pollution in this unique basin.

2 Methodology

2.1 Sampling sites

$PM_{2.5}$ samples were collected at two urban sites, one in Chengdu and another in Chongqing, the two largest cities in Sichuan Basin, southwest China (Wang et al., 2017). The two sampling sites are located 260 km apart (Fig. 1). The sampling site in Chengdu (CD) is located on the roof of a sixth floor building in the Sichuan Academy of Environmental Science (104º4′ E, 30º37′ N) with no large surrounding industries but heavy traffic. The closest main road (Renmin South road of Chengdu) is about 20 m east of the samling site. The sampling site in Chongqing (CQ) is located on the rooftop of Chongqing Monitoring Center (106º30′ E, 29º37′ N). The highway G50 is 250 m away from this sampling site. The two selected sampling sites are considered to represent typical urban environment in their respective cities without the influence of local point sources from industry activities.

Atmos. Chem. Phys. Discuss., doi:10.5194/acp-2017-258, 2017
Manuscript under review for journal Atmos. Chem. Phys.
Discussion started: 10 April 2017

Atmospheric Chemistry and Physics Discussions

2.2 Sample collection

Daily (23-h) integrated $PM_{2.5}$ samples were collected in four months, each in a different season: autumn (23 October to 18 November, 2014), winter (6 January to 2 February, 2015), spring (2 to 29 April, 2015), and summer (2 to 30 July, 2015). At both sites, $PM_{2.5}$ samples were collected in parallel on Teflon filters (Whatman Corp., 47 mm) and quartz filters (Whatman Corp., 47 mm) and used for different chemical analyses. At the CD site, $PM_{2.5}$ sampling was carried out using an versatile air pollutant sampler (Wang et al., 2017). One channel was used to load $PM_{2.5}$ sample on Teflon filter for mass and trace elements anlysis and the other one was equipped with quatz filter for water-soluble inorganic ions and carbonaceous components analysis. The sampler was running at 15 L min^{-1} for each channel. At the CQ site, a low-volume aerosol sampler (BGI Corp., frmOmni, USA) operating at a flow rate of 5 L min^{-1} was used to collect $PM_{2.5}$ samples on Teflon filter, and another sampler (Thermo Scientific Corp. Partisol 2000i, USA) with a flow rate of 16.7 L min^{-1} was used to collect $PM_{2.5}$ samples on quartz filter.

Before sampling, all the quartz filters were preheated at 450°C for 4 h to remove the organic compounds. All sampled filters were stored in clean Petri slides in the dark and at -18°C until analysis to prevent the evaporation of volatile compounds. Before and after sample collection, all the Teflon filters were weighted at least three times using an microbalance (Sartorius, ME 5-F, Germany) after their stabilization for 48 h under controlled conditions (temperature: 20~23°C, relative humidity: 45~50%). Differences among replicate weights were mostly less than 15 μg for each sample.

2.3 Chemical analysis

For the analysis of water-soluble inorganic ions, a quarter of each quartz filter was first extracted using ultrapure water in an ultrasonic bath for 30 min, and then filtered through a 0.45 μm pore syringe filter. Anions (SO_4^{2-}, NO_3^- and Cl^-) and cations (Na^+, NH_4^+, K^+, Mg^{2+} and Ca^{2+}) were determined using ion chromatograph (Dionex Corp., Dionex 600, USA). Anions were separated using AS11-HC column with 30 mM KOH as an eluent at a flow rate of 1.0 ml min^{-1}. Cations were determined using CS12A column with 20 mM MSA (methanesulfonic acid) at a flow rate of 1.0 ml min^{-1}. Individual standard solutions of all investigated anions and cations (1000 mg L^{-1}, o2si, USA) were diluted to construct the calibration curves. The correlation coefficients of the linear regression of the standard curves were all above 0.999. Field blanks were prepared and analyzed together with the samples and then subtracted from the samples. The concentrations of the water-soluble inorganic ions in the field blanks were in the range of

0.008-0.13 μg m^{-3}. The relative standard deviation of each ion was better than 8% for the reproducibility test.

Organic carbon (OC) and elemental carbon (EC) were measured by thermal-optical reflectance (TOR) method using a DRI OC/EC analyzer (Atmoslytic Inc., USA). The methodology for OC/EC analysis was based on TOR method as described in Chow et al. (2007). For calibration and quality control, measurement with filter blank, standard sucrose solution and replicate analysis were performed. Blank corrections were performed by subtracting the blank values from the sampled ones. The concentration of EC in field blanks was zero while OC were below 0.7 μg C cm^{-2}. The repeatability was better than 15%.

The elements including Al, Si, Ca, Fe, and Ti were analyzed on Teflon filter using X-ray fluorescence analyzer (Epsilon 5ED-XRF, PAN'alytical Corp., Netherlands), the QA/QC procedures of the XRF analysis have been described in Cao et al. (2012).

The gaseous species were continuously measured by a set of online gas analyzers, including EC9850 SO_2 analyzer, 9841 $NO/NO_2/NO_x$ analyzer, 9830 CO analyzer, and 9810 O_3 analyzer (Ecotech Corp., Australia) at the CD site, and Thermo 42i $NO/NO_2/NO_x$ analyzer, 43i SO_2 analyzer, 48i CO analyzer, and 49i O_3 analyzer (Thermo Scientific Corp., USA) at the CQ site. The mass concentration of $PM_{2.5}$ was automatically measured by online particulate monitor instruments (BAM1020, Met one Corp., USA, at CD and 5030 SHARP, Thermo Scientific Corp, USA, at CQ). Hourly meteorological parameters, including ambient temperature (T), relative humidity (RH), wind speed (WS) and direction, barometric pressure (P), and solar radiation (SR), were obtained from an automatic weather station at each site.

2.4 Data analysis

The EC-tracer method has been widely used to estimate SOC (Turpin and Huntzicker, 1995; Castro et al., 1999), which can be expressed as

$$POC=(OC/EC)_{prim} \times EC \quad (1)$$

$$SOC=OC-POC \quad (2)$$

Where POC, SOC and OC represent estimated primary OC, secondary OC and measured total OC, respectively. $(OC/EC)_{min}$ was simplified as the $(OC/EC)_{prim}$ to estimate SOC in this study. $(OC/EC)_{min}$ was 2.4, 2.6, 1.6 and 2.2 in autumn, winter, spring and summer at CD, respectively, and 1.9, 2.8, 1.1 and 1.5 at CQ. The estimated SOC was only an approximation with uncertainties, e.g., from influence

Atmos. Chem. Phys. Discuss., doi:10.5194/acp-2017-258, 2017
Manuscript under review for journal Atmos. Chem. Phys.
Discussion started: 10 April 2017

Atmospheric Chemistry and Physics Discussions

of biomass burning (Ding et al., 2012).

The coefficient of divergence (COD) has been used to evaluate the spatial similarity of chemical compositions at different sites (Wongphatarakul et al., 1998; Qu et al., 2015), which is defined as

$$COD_{jk} = \sqrt{\frac{1}{p}\sum_{1}^{p}\left(\frac{x_{ij}-x_{ik}}{x_{ij}+x_{ik}}\right)^2} \quad (3)$$

Where x_{ij} and x_{ik} represent the average concentration for a chemical component i at site j and k, respectively, p is the number of chemical components. Generally, a COD value lower than 0.2 indicates a relatively similarity of spatial distribution.

2.5 Geographical origins of $PM_{2.5}$

72-h air mass back trajectories were generated based on the Hybrid Single Particle Lagrangian Integrated Trajectory (HYSPLIT) model using 40 km gridded meteorological data (GDAS 40 km) for $PM_{2.5}$ measurements from October 2014 to July 2015 at both sites. Four trajectories at 04:00, 10:00, 16:00, and 22:00 UTC every day with the starting height of 300 m above ground level were calculated (Squizzato and Masiol, 2015). The trajectories coupled with daily $PM_{2.5}$ concentrations were used for PSCF analysis, with the threshold criterion in PSCF analysis being set at the upper 50% of $PM_{2.5}$. The trajectory covered area was in the range of 20-45º N and 90-120º E and divided into 0.5º×0.5º grid cells.

3 Results and discussion

3.1 Overview of $PM_{2.5}$ mass concentrations and major components

Table 1 presents seasonal and annual mean concentrations of $PM_{2.5}$ and its major chemical components at CD and CQ during the sampling periods. Daily $PM_{2.5}$ ranged from 11.6 to 224.7 μg m^{-3} with annual average being 67.0 ± 43.4 μg m^{-3} at CD site and 70.9 ± 41.4 μg m^{-3} at CQ site. The annual average values were about two times of the NAAQS annual limit. Secondary inorganic aerosol (SNA, the sum of SO_4^{2-}, NO_3^- and NH_4^+) and carbonaceous species together represented more than 70% of $PM_{2.5}$ at both sites (Fig. 2). The annual mean concentrations of the total SNA were 27.6 and 26.5 μg m^{-3} at CD and CQ, respectively, contributing 41.1% and 37.4% of $PM_{2.5}$. Among these, SO_4^{2-}, NO_3^- and NH_4^+ were 11.2, 9.1, and 7.2 μg m^{-3}, respectively, or 16.8%, 13.6% and 10.8% of $PM_{2.5}$ mass at CD, and 12.2, 7.7 and 6.6 μg m^{-3} or 17.2%, 10.9% and 9.2% of $PM_{2.5}$ mass at CQ. Organic matters (OM), estimated from OC by using a conversion factor of 1.6 to account for other elements present in organic

compounds (Turpin and Lim, 2001), were the most abundant species in $PM_{2.5}$, accounting for 26.1% and 29.6% of $PM_{2.5}$ mass at CD and CQ, respectively. In contrast, EC only comprised of around 6% at both sites. The annual mean OC and EC at CQ were 20% and 25% higher than those at CD. Fine soil (FS) can be estimated by summing the oxides of the elements mainly associated with soil, i.e., Al_2O_3, SiO_2, CaO, FeO, Fe_2O_3, and TiO_2 (Huang et al., 2014). The annual mean concentration of FS at CQ was 6.7 μg m^{-3} (or 9.5% of $PM_{2.5}$), which was about two times of that at CD (3.8 μg m^{-3} or 5.7% of $PM_{2.5}$). The minor components such as K^+ and Cl^- constituted less than 5% of $PM_{2.5}$. The unaccounted portion of $PM_{2.5}$ reached 18.3% at CD and 15.3% at CQ, which was likely related to the uncertainties in the multiplication factor used for estimation of OM and FS, other unidentified species, and measurement uncertainties.

3.2 Seasonal variations

Figure 3 shows the seasonal variations of mass concentrations of $PM_{2.5}$ and its major chemical components at CD and CQ sites. Seasonal-average $PM_{2.5}$ was the highest in winter at both sites, which was 1.8-2.5 times of those in the other seasons. Besides the high emissions of SO_2 and NO_x in winter, stagnant air condition with frequent calm winds and low boundary layer height was another major cause of the highest $PM_{2.5}$ in this season (Chen and Xie, 2013). Seasonal differences among the other three seasons were generally small, e.g., less than 40%. All $PM_{2.5}$ components but FS followed the seasonal pattern of $PM_{2.5}$ with the highest concentrations in winter, but with subtle differences. The majority of the components showed a summer minimum, but not SO_4^{2-}. The minimum of OC at CD and FS at CQ appeared in spring and autumn, respectively. Higher SO_4^{2-} concentrations in summer were likely due to the enhanced photochemical reactions associated with higher temperature and stronger solar radiation in summer. It is also noted that the seasonal variations in NO_3^- were much larger than those in SO_4^{2-} and NH_4^+, which can be explained by the enhanced formation of NO_3^- under high relative humidity in winter, and volatility of NH_4NO_3 in summer (Pathak et al., 2009; Quan et al., 2015; Squizzato et al., 2013). In addition, thermodynamically driven behavior of NH_4NO_3 was another factor for the lower NO_3^- concentrations in summer (Wang et al., 2016; Kuprov et al., 2014). High levels of Cl^- and K^+ in winter and of FS in spring should be caused by biomass burning or spring dust storms (Tao et al. 2013, 2014).

Both OC and EC showed the highest concentrations in winter at CD and CQ, whereas seasonal differences of those carbonaceous components were less distinct in other seasons, e.g. the variations of OC and EC among other three seasons were less than 30%. Seasonal average SOC was unexpectedly

the highest in winter at both sites, different from the anticipated high value in summer in consideration of strong photochemical reaction. Condensation of semi-volatile organic aerosols in winter seemed to play a larger role than photochemical reaction in summer, knowing that low temperature favors condensation process (Sahu et al., 2011; Cesari et al., 2016). Although high O_3 and strong solar radiation condition in summer was conducive to strong photochemical reactions, high temperature favors gas-particle partitioning in the gaseous phase and thus limited the increase of SOC (Strader et al., 1999).

The seasonal relative contributions of major chemical component to $PM_{2.5}$ are shown in Fig. 2. The seasonal average contributions of SNA to $PM_{2.5}$ only varied within a small range from 39.5% to 43.2% at CD, whereas in a relatively larger range from 31.0% in summer to 37.1-41.5% in other seasons at CQ. The smaller contribution in summer at CQ was mainly due to the lower NO_3^- concentrations. At both CD and CQ, NO_3^- and NH_4^+ showed the highest contributions in winter and the lowest one in summer, whereas an opposite trend was found for SO_4^{2-}. The contributions of carbonaceous components (the sum of OC and EC) generally followed the seasonal patterns of SNA, accounting for 26.7-38.8% of $PM_{2.5}$ mass. Among these, OM showed the lowest fractions in $PM_{2.5}$ in spring (21.1%) at CD and highest value in winter (33.6%) at CQ, while the percentages of OM in other seasons were similar at both sites, around 27%. The seasonal variations of EC fractions were not obvious, with a slightly higher value in spring. The highest contributions from FS was more than 10%, appeared in spring at both sites.

3.3 Site differences

A comparison between the two sites in terms of seasonal-average concentrations of major chemical components are shown in Fig. 4. Despite the 260 km distance between the two sampling sites, a moderate similarity was observed in autumn, winter and spring on the basis of low COD values (0.15-0.18), indicating the regional-scale $PM_{2.5}$ pollution pattern in Sichuan Basin and the similarity in major emission sources for both sites. However, it is worth to note that several components differed by up to a factor of 2.5 in their season-average concentrations, e.g. OC and EC in winter and spring, and Cl^- and FS in all the four seasons. These discrepancies were partly caused by the different atmospheric chemical processes and local sources between the two sites on certain days. In summer, the differences for several major chemical components (FS, OC, SO_4^{2-}, NO_3^-, EC) between the two sites were larger than in other seasons, causing the high COD value (0.33) in this season.

Good correlations between the two sites were found for daily SNA, OC, EC and K^+ concentrations

Atmos. Chem. Phys. Discuss., doi:10.5194/acp-2017-258, 2017
Manuscript under review for journal Atmos. Chem. Phys.
Discussion started: 10 April 2017

in autumn, winter and spring (Table 2). However, for NO_3^-, a significant correlation was identified only in autumn, likely due to the strong impact of local vehicle emissions and the subsequent atmospheric processes forming NO_3^-. Similarly, a moderate correlation was observed just in winter for both Cl^- and FS. In summer, weak or no correlations were identified between the two sites for almost all chemical components. Therefore, there existed a fairly uniform distribution of most major components in $PM_{2.5}$ throughout the basin in all the seasons except summer.

3.4 Chemical characteristics of $PM_{2.5}$ on clean and polluted days

3.4.1 Key chemical species causing polluted days

To explore the major chemical pollutants responsible for polluted days, daily $PM_{2.5}$ data were categorized into two groups, i.e. clean days and polluted days based on $PM_{2.5}$ concentrations below and above the NAAQS guideline value of 75 μg m^{-3}, respectively. 34 and 31 polluted days were counted at CD and CQ site, respectively, accounting for 30.4% and 28.6% of the entire sampling days. The number of polluted days at CD was 8, 21, 4 and 1 in autumn, winter, spring and summer, accounting for 29.6%, 75%, 14.3% and 3.4% of the total sampling days in each season, respectively, and at CQ they were 4, 19, 6 and 2, accounting for 14.8%, 67.9%, 21.4% and 6.9%. Note that these numbers were only from one-month (around 28 days) sampling in each season. Considering the similar meteorological conditions and pollution levels during autumn and spring, these two seasons were combined together and was referred to as the warm season, while winter was referred to as the cold season. Because of the very small number of polluted days in summer at both sites, the $PM_{2.5}$ data in this season were not discussed.

$PM_{2.5}$ concentrations increased dramatically on polluted days compared to clean days (Fig. 5). For example, $PM_{2.5}$ concentrations were more than doubled on polluted days during the entire sampling periods at both sites. The two dominant groups of components in $PM_{2.5}$, SNA and OC, were 2.5-2.8 times higher on polluted days in both cold and warm seasons at CD. However, larger variations were found at CQ with SNA increased by 2.7 and 1.7 times, and OM by 3.4 and 2.1 times in the cold and warm season, respectively. Thus, while the enhancement of SNA and OC on polluted days were similar at CD, OC increased much more at CQ, indicating some different contributing factors to the high $PM_{2.5}$ pollution at the two sites. Pollutants accumulation under stagnant meteorological conditions might be a main factor at CD based on the similar magnitudes of the enhancements of $PM_{2.5}$ and its dominant

components, while additional processes should have increased OC more than other components at CQ.

In the cold season, the percentage contributions of SNA to $PM_{2.5}$ were similar on clean and polluted days, 38-41% at both sites (Fig. S1). However, the percentage contribution of OM to $PM_{2.5}$ decreased from 30.1% on clean days to 27.5% on polluted days at CD, and increased from 26.9% to 34.9% at CQ. A different pattern was seen in the warm season, with no significant variations of OM fractions in $PM_{2.5}$ between the clean and polluted days at either site, but an increased SNA contribution by around 7% at CD and decreased contribution by 14% at CQ. The percentage contributions of SNA and OM to $PM_{2.5}$ discussed above were different from those found in eastern coastal China and North China Plain, where considerable increases were found for SNA and decreases for OM on polluted days than clean days (Tan et al., 2009; Wang et al., 2015; Quan et al., 2014; Zhang et al., 2015a; Zhang et al., 2016; Cheng et al., 2015). This emphasized again the unique characteristics of $PM_{2.5}$ pollution in Sichuan Basin due to its particular topography and meteorological conditions.

Concentrations of the individual SNA species (SO_4^{2-}, NO_3^- and NH_4^+) increased by a factor of 1.2-3.3 on polluted days compared to clean days in all the cases (Fig. 5). But the percentage contributions differed among the species as NO_3^- increased and SO_4^{2-} decreased on polluted days. The concentration of FS increased slightly at CD (less than 3 μg m^{-3}) but significantly (from 5.4 on clean days to 14.7 μg m^{-3} on polluted days) at CQ in warm season. The percentage contribution of FS to $PM_{2.5}$ reached 15.3% on polluted days at CQ in warm season.

3.4.2 Transformation mechanisms of secondary aerosols

Meteorological conditions, atmospheric chemical processes and long-range transport are all responsible for $PM_{2.5}$ accumulation on polluted days (Zheng et al., 2015b). CO and EC are directly emitted from combustion processes and are not very reactive, thus their concentrations in the air are strongly controlled by meteorological parameters within a relatively short period. Both CO and EC concentrations increased on polluted days (Fig. 5 and Fig. S2), suggesting the important role the meteorological condition played on $PM_{2.5}$ accumulation. As expected, very weak winds (less than 0.7 m s^{-1}) were observed on polluted days, which hindered the pollutants horizontal transport. CO can be considered as a reference pollutant species whose temporal variations were mainly from the impact of meteorological conditions. The impact of other factors on other pollutants can thus be explored by scaling the concentrations of other pollutants to that of CO. For example, $PM_{2.5}$ was enhanced by a factor of 2.0-2.7 on polluted days than clean days in the two seasons and at the two sites, but the

Atmos. Chem. Phys. Discuss., doi:10.5194/acp-2017-258, 2017
Manuscript under review for journal Atmos. Chem. Phys.
Discussion started: 10 April 2017

Atmospheric Chemistry and Physics Discussions

CO-scaled $PM_{2.5}$ only showed an enhancement of a factor of 1.5-1.8 (Fig. 6), and the latter values were likely from the enhanced secondary aerosol formation.

As shown in Fig. 6, the CO-scaled SNA was 60-90% higher on polluted days with individual species 40-120% higher (except in the warm season at CQ), even though their gaseous precursor (SO_2 and NO_2, no data for NH_3) were only less than 30% higher. This suggests stronger chemical transformation from gaseous precursors to particle formation on polluted days. Sulfur oxidation ratio (SOR = $n\text{-}SO_4^{2-}/(n\text{-}SO_4^{2-}+n\text{-}SO_2)$) and nitrogen oxidation ratio (NOR = $n\text{-}NO_3^-/(n\text{-}NO_3^-+n\text{-}NO_2)$) were defined to evaluate the degree of secondary transformation (*n* refers to as the molar concentration). In the cold season, NOR increased from 0.09 on clean days to 0.16 on polluted days at CD and from 0.07 to 0.14 at CQ. SOR increased only slightly, from 0.31 to 0.35 at CD and 0.28 to 0.35 at CQ. In the warm season, NOR and SOR exhibited a similar pattern as those in the cold season with the exception of NOR at CQ, which might be related to the high temperature in the warm season. The CO-scaled SOC increased by a factor of 2.6 and 1.5 on polluted days in the cold and warm season at CQ, but no significant change or decrease was found at CD. Moreover, increased SOC/OC only occurred at CQ in the cold season (Fig. 6). The different pattern in SOC (or SOC/OC) than SNA (or SOR and NOR) suggests that secondary organic aerosols (SOA) production is of less important than SNA production in most occasions except in the cold season at CQ.

The formation mechanisms of secondary aerosols were further explored based on the diurnal variations of their gaseous precursors and the relevant meteorological parameters. Considering the different characteristics of $PM_{2.5}$ pollution, the polluted days were further divided into moderate polluted days ($75 < PM_{2.5} \leq 150$ μg m^{-3}) and heavy polluted days ($PM_{2.5} > 150$ μg m^{-3}). Figure 7 and Fig. S2 describe the diurnal variations of T, RH, WS, SR, NO, CO, SO_2, NO_2 and O_3 concentrations in the cold season at CD and CQ. Most gaseous species except O_3 showed relatively higher concentrations on polluted days, but exhibited different diurnal patterns under different pollution levels. For example, NO and CO both reached their peak values at around 10:00 am, consistent with the morning traffic rush hours (Fig. S2). For SO_2 and NO_2, similar diurnal variations were seen on clean and moderate polluted days, but a different one on heavy polluted days, with the latter having long-lasting (from 12:00 to 18:00 pm) high concentrations likely caused by transport as supported by stronger afternoon winds on these days (Fig. 7). O_3 showed a typical diurnal variation with a peak value at around 16:00 pm. Daytime (11:00-20:00 LT) O_3 was much higher on moderate polluted days, but slightly lower on heavy

Atmos. Chem. Phys. Discuss., doi:10.5194/acp-2017-258, 2017
Manuscript under review for journal Atmos. Chem. Phys.
Discussion started: 10 April 2017

polluted days compared to those on clean days. Aerosols were generally considered as a constrain factor to O_3 production due to their absorbing or scattering the UV radiation, which would reduce solar radiation and consequently decrease the photochemical activity and O_3 levels (Zhang et al., 2015b; Zheng et al., 2015b; Tian et al., 2016). The O_3 data on heavy polluted days seemed to support this hypothesis, but not those on moderate polluted days. The diurnal variations of O_3 tracked the pattern of solar radiation (Fig. S2), which might be associated with the special climate characteristics in Chengdu with extremely low annual sunshine totals and mostly overcast days, especially in winter. As a result, the impact of weather conditions on solar radiation might overwhelm that of aerosol pollution at CD and caused unusual diurnal variations of O_3 and solar radiation. In the warm season, no heavy $PM_{2.5}$ pollution occurred at CD and CQ, and the diurnal patterns of gaseous precursors and meteorological parameters were similar as those in the cold season (Fig. 8 and Fig. S3).

Besides the well-known photochemical processes forming SO_4^{2-} and NO_3^- (Stockwell and Calvert, 1983; Blitz et al., 2003; Calvert and Stockwell, 1983), heterogeneous reactions might also be important formation mechanisms for these SNA species (Quan et al., 2015; Zheng et al., 2015a; Zhao et al., 2013b). Similarly, SOA is mainly formed through photochemical oxidation of primary VOCs followed by condensation of SVOC onto particles as well as through aqueous-phase reactions (Ervens et al., 2011). While photochemical reactions are mostly influenced by temperature and solar radiation, heterogeneous reactions are associated with high RH. Meteorological conditions and O_3 levels associated with different pollution levels suggest that gas-phase oxidation reaction was likely the major formation mechanism of secondary aerosols on moderate polluted days (high O_3 levels and SR, low RH) while heterogeneous reactions likely played a more important role on heavy polluted days (low O_3 levels and slightly higher RH). This hypothesis needs further verification using high-resolution data.

3.4.3 Impact of NH_3 amount and RH on NO_3^- concentrations

In Sect. 3.4.2, it was found that the CO-scaled NO_3^- increased dramatically in the cold season but decreased in the warm season on polluted days at CQ. To explain the different season patterns, major factors affecting NO_3^- are explored, including NH_3 levels and RH. The neutralization ratio (NR) is defined as

$$NR = \frac{[NH_4^+]}{2[SO_4^{2-}]+[NO_3^-]} \quad (4)$$

Where the concentrations of NH_4^+, SO_4^{2-} and NO_3^- were expressed as molar concentrations. NR in cold

season ranged from 1.0 to 1.2 at the two sites, indicating fully neutralization of SO_4^{2-} and NO_3^- by NH_3. In this case, NH_3 was not a limiting factor for NO_3^-. NR in the warm season was 1.05 at CD, but less than 1.0 (0.94-0.95) at CQ. NH_3 seemed to be a limiting factor for NO_3^- formation at CQ on both clean and polluted days in the warm season. Although NH_4^+ increased on polluted days (by 30% based on CO-scaled concentrations), SO_4^{2-} increased even more (by 60% based on scaled concentration), resulting in incomplete neutralization of NO_3^- and little variations of its concentrations.

Another consideration is the thermodynamic equilibrium between particulate NH_4NO_3 and gaseous HNO_3, which depends on temperature and RH. Kuprov et al. (2014) found that the equilibrium would be shifted toward the particulate phase when RH was above the deliquescence relative humidity (DRH) of NH_4NO_3, and the dissociation constant decreased to about an order of magnitude when RH was above 75%. As shown in Fig. S4, on polluted days, RH was lower than DRH most of the time in the warm season at CQ estimated according to Mozurkewich (1993), which explains the lower NO_3^- concentrations. In contrast, RH was above the DRH most of the time at CD. Thus, despite similar concentrations of SO_4^{2-} and NH_4^+ between CD and CQ in summer, NO_3^- was 50% lower at CQ than that at CD due to the lower ambient RH at CQ.

3.5 Geographical origins causing high $PM_{2.5}$ pollution

PSCF analysis was applied to investigate the potential source regions contributing to high $PM_{2.5}$ pollution (Fig. 9). Basically, all the major source areas for high $PM_{2.5}$ were distributed within the Basin. Long-range transports normally occurred in North Plain and eastern coastal regions were not observed at CD and CQ site (Zhao et al., 2015; Zhang et al., 2013). At CD, the major source areas in the cold season included the areas of the northeastern, southeastern and southern Chengdu and in some areas of Chongqing, and in warm season included areas scattered between Chengdu and Chongqing (e.g., Neijiang) besides the area south of Chengdu. At CQ in the cold season, the northeast area of Chongqing was identified as strong sources, where a number of industries were located, such as Changshou chemical industrial ozone. In the warm season, the areas of the southern Chongqing were also found to be potential sources. Overall, $PM_{2.5}$ pollution at CQ was characterized by significant local contribution from major sources located in or nearby Chongqing. In contrast, regional transport in Sichuan Basin from southeast, south and southwest of Chengdu had a major impact on $PM_{2.5}$ pollution at CD.

4 Conclusions

Seasonal patterns, formation mechanisms, and sources origins of $PM_{2.5}$ at the two megacities in Sichuan Basin were explored using chemically resolved daily $PM_{2.5}$ samples collected in four consecutive seasons. On about 30% of the days, daily $PM_{2.5}$ exceeded NAAQS, with SNA and OC concentrations 1.7-2.8 and 2.1-3.4 times, respectively, higher than those on clean days. The percentage contributions of SNA and OM to $PM_{2.5}$ mass only differed slightly between polluted and clean days at CD, while it increased significantly for OM at CQ in cold season. This phenomenon was different from those found in the other regions of China, implying the unique roles played by local topography, meteorology, and emissions sources in this region. Most chemical components of $PM_{2.5}$ exhibited the highest concentrations in the winter (with exception of FS) and the lowest in the summer (with exception of SO_4^{2-}). The site differences in $PM_{2.5}$ and SNA between CD and CQ were not significant in all the seasons except in the summer, while higher OC and FS concentrations were observed at CQ than at CD in most seasons. The different diurnal patterns of gaseous precursors and meteorological parameters under different $PM_{2.5}$ level implied the more important roles of heterogeneous transformation on the heavy polluted days. The ammonia-limited and high temperature conditions also played a critical role in low NO_3^- levels in the warm season at CQ. Major sources of $PM_{2.5}$ were concentrated in Chengdu, Chongqing, and the areas in between, with the regional sources affecting more at CD site and the local emissions at CQ site. Future studies should aim to combine high-resolution $PM_{2.5}$ data and at suburban and rural locations to gain a thorough understanding of $PM_{2.5}$ sources and formation mechanisms.

Competing interests. The authors declare that they have no conflict of interest.

Acknowledgements. This work was supported by the National Natural Science Foundation of China (No. 41405027, 41375123, and 41403089), the "Strategic Priority Research Program" of the Chinese Academy of Sciences (No. KJZD-EW-TZ-G06), the West Action Plan of the Chinese Academy of Science (No. KZCX2-XB3-14), and Chongqing Science and Technology Commission (No. cstc2014yykfC20003, cstckjcxljrc13). We are grateful to Yumeng Zhu and Jun Wang for sample collection.

Reference

Anderson, G. B., Krall, J. R., Peng, R. D., and Bell, M. L.: Is the Relation Between Ozone and Mortality Confounded by Chemical Components of Particulate Matter? Analysis of 7 Components in 57 US Communities, Am J Epidemiol, 176, 726-732, 10.1093/aje/kws188, 2012.

Baumer, D., Vogel, B., Versick, S., Rinke, R., Mohler, O., and Schnaiter, M.: Relationship of visibility, aerosol optical thickness and aerosol size distribution in an ageing air mass over South-West Germany, Atmos Environ, 42, 989-998, 10.1016/j.atmosenv.2007.10.017, 2008.

Blitz, M. A., Hughes, K. J., and Pilling, M. J.: Determination of the high-pressure limiting rate coefficient and the enthalpy of reaction for OH+SO2, J Phys Chem A, 107, 1971-1978, 10.1021/jp026524y, 2003.

Calvert, J. G., and Stockwell, W. R.: Acid Generation in the Troposphere by Gas-Phase Chemistry, Environ Sci Technol, 17, A428-A443, DOI 10.1021/es00115a002, 1983.

Cao, J. J., Wang, Q. Y., Chow, J. C., Watson, J. G., Tie, X. X., Shen, Z. X., Wang, P., and An, Z. S.: Impacts of aerosol compositions on visibility impairment in Xi'an, China, Atmos Environ, 59, 559-566, 10.1016/j.atmosenv.2012.05.036, 2012.

Castro, L. M., Pio, C. A., Harrison, R. M., and Smith, D. J. T.: Carbonaceous aerosol in urban and rural European atmospheres: estimation of secondary organic carbon concentrations, Atmos Environ, 33, 2771-2781, Doi 10.1016/S1352-2310(98)00331-8, 1999.

Cesari, D., Donateo, A., Conte, M., Merico, E., Giangreco, A., Giangreco, F., and Contini, D.: An inter-comparison of $PM_{2.5}$ at urban and urban background sites: Chemical characterization and source apportionment, Atmos Res, 174, 106-119, 10.1016/j.atmosres.2016.02.004, 2016.

Chen, Y., and Xie, S. D.: Long-term trends and characteristics of visibility in two megacities in southwest China: Chengdu and Chongqing, J Air Waste Manage, 63, 1058-1069, 10.1080/10962247.2013.791348, 2013.

Cheng, Y., He, K. B., Du, Z. Y., Zheng, M., Duan, F. K., and Ma, Y. L.: Humidity plays an important role in the $PM_{2.5}$ pollution in Beijing, Environ Pollut, 197, 68-75, 10.1016/j.envpol.2014.11.028, 2015.

Chow, J. C., Watson, J. G., Chen, L. W. A., Chang, M. C. O., Robinson, N. F., Trimble, D., and Kohl, S.: The IMPROVE-A temperature protocol for thermal/optical carbon analysis: maintaining consistency with a long-term database, J Air Waste Manage, 57, 1014-1023, 10.3155/1047-3289.57.9.1014, 2007.

Ding, X., Wang, X. M., Gao, B., Fu, X. X., He, Q. F., Zhao, X. Y., Yu, J. Z., and Zheng, M.: Tracer-based estimation of secondary organic carbon in the Pearl River Delta, south China, J Geophys Res-Atmos, 117, Artn D0531310.1029/2011jd016596, 2012.

Ervens, B., Turpin, B. J., and Weber, R. J.: Secondary organic aerosol formation in cloud droplets and aqueous particles (aqSOA): a review of laboratory, field and model studies, Atmos Chem Phys, 11, 11069-11102, 10.5194/acp-11-11069-2011, 2011.

Fu, X. X., Wang, X. M., Hu, Q. H., Li, G. H., Ding, X., Zhang, Y. L., He, Q. F., Liu, T. Y., Zhang, Z., Yu, Q. Q., Shen, R. Q., and Bi, X. H.: Changes in visibility with $PM_{2.5}$ composition and relative humidity at a background site in the Pearl River Delta region, J Environ Sci-China, 40, 10-19, 10.1016/j.jes.2015.12.001, 2016.

Hitzenberger, R., Berner, A., Giebl, H., Kromp, R., Larson, S. M., Rouc, A., Koch, A., Marischka, S., and Puxbaum, H.: Contribution of carbonaceous material to cloud condensation nuclei concentrations in European background (Mt. Sonnblick) and urban (Vienna) aerosols, Atmos Environ, 33, 2647-2659, Doi 10.1016/S1352-2310(98)00391-4, 1999.

Huang, X. H. H., Bian, Q. J., Ng, W. M., Louie, P. K. K., and Yu, J. Z.: Characterization of $PM_{2.5}$ Major Components and Source Investigation in Suburban Hong Kong: A One Year Monitoring Study, Aerosol Air Qual Res, 14, 237-250, 10.4209/aaqr.2013.01.0020, 2014.

Ji, D. S., Zhang, J. K., He, J., Wang, X. J., Pang, B., Liu, Z. R., Wang, L. L., and Wang, Y. S.: Characteristics of atmospheric organic and elemental carbon aerosols in urban Beijing, China, Atmos Environ, 125, 293-306, 10.1016/j.atmosenv.2015.11.020, 2016.

438 Kuprov, R., Eatough, D. J., Cruickshank, T., Olson, N., Cropper, P. M., and Hansen, J. C.: Composition and secondary
439 formation of fine particulate matter in the Salt Lake Valley: Winter 2009, J Air Waste Manage, 64, 957-969,
440 10.1080/10962247.2014.903878, 2014.
441 Larssen, T., Lydersen, E., Tang, D. G., He, Y., Gao, J. X., Liu, H. Y., Duan, L., Seip, H. M., Vogt, R. D., Mulder, J., Shao, M.,
442 Wang, Y. H., Shang, H., Zhang, X. S., Solberg, S., Aas, W., Okland, T., Eilertsen, O., Angell, V., Liu, Q. R., Zhao, D. W.,
443 Xiang, R. J., Xiao, J. S., and Luo, J. H.: Acid rain in China, Environ Sci Technol, 40, 418-425, Doi 10.1021/Es0626133,
444 2006.
445 Lepeule, J., Laden, F., Dockery, D., and Schwartz, J.: Chronic Exposure to Fine Particles and Mortality: An Extended
446 Follow-up of the Harvard Six Cities Study from 1974 to 2009, Environ Health Persp, 120, 965-970, 10.1289/ehp.1104660,
447 2012.
448 Li, B., Zhang, J., Zhao, Y., Yuan, S. Y., Zhao, Q. Y., Shen, G. F., and Wu, H. S.: Seasonal variation of urban carbonaceous
449 aerosols in a typical city Nanjing in Yangtze River Delta, China, Atmos Environ, 106, 223-231,
450 10.1016/j.atmosenv.2015.01.064, 2015.
451 Lu, Z., Zhang, Q., and Streets, D. G.: Sulfur dioxide and primary carbonaceous aerosol emissions in China and India,
452 1996-2010, Atmos Chem Phys, 11, 9839-9864, 10.5194/acp-11-9839-2011, 2011.
453 Mahowald, N.: Aerosol Indirect Effect on Biogeochemical Cycles and Climate, Science, 334, 794-796,
454 10.1126/science.1207374, 2011.
455 Mengting, G., Xuhu, C., and Yu, S.: Characteristics of Low Wind-Speed Meteorology in China, Acta Scientiarum
456 Naturalium Universitatis Pekinensis, 52, 219-226, 2016.
457 Mozurkewich, M.: The Dissociation-Constant of Ammonium-Nitrate and Its Dependence on Temperature,
458 Relative-Humidity and Particle-Size, Atmos Environ a-Gen, 27, 261-270, Doi 10.1016/0960-1686(93)90356-4, 1993.
459 Paraskevopoulou, D., Liakakou, E., Gerasopoulos, E., and Mihalopoulos, N.: Sources of atmospheric aerosol from long-term
460 measurements (5 years) of chemical composition in Athens, Greece, Sci Total Environ, 527, 165-178,
461 10.1016/j.scitotenv.2015.04.022, 2015.
462 Pathak, R. K., Wu, W. S., and Wang, T.: Summertime $PM_{2.5}$ ionic species in four major cities of China: nitrate formation in
463 an ammonia-deficient atmosphere, Atmos Chem Phys, 9, 1711-1722, 2009.
464 Qu, W. J., Wang, J., Zhang, X. Y., Wang, D., and Sheng, L. F.: Influence of relative humidity on aerosol composition:
465 Impacts on light extinction and visibility impairment at two sites in coastal area of China, Atmos Res, 153, 500-511,
466 10.1016/j.atmosres.2014.10.009, 2015.
467 Quan, J. N., Tie, X. X., Zhang, Q., Liu, Q., Li, X., Gao, Y., and Zhao, D. L.: Characteristics of heavy aerosol pollution during
468 the 2012-2013 winter in Beijing, China, Atmos Environ, 88, 83-89, 10.1016/j.atmosenv.2014.01.058, 2014.
469 Quan, J. N., Liu, Q., Li, X., Gao, Y., Jia, X. C., Sheng, J. J., and Liu, Y. G.: Effect of heterogeneous aqueous reactions on the
470 secondary formation of inorganic aerosols during haze events, Atmos Environ, 122, 306-312,
471 10.1016/j.atmosenv.2015.09.068, 2015.
472 Ramanathan, V., and Feng, Y.: Air pollution, greenhouse gases and climate change: Global and regional perspectives, Atmos
473 Environ, 43, 37-50, 10.1016/j.atmosenv.2008.09.063, 2009.
474 Sahu, L. K., Kondo, Y., Miyazaki, Y., Pongkiatkul, P., and Oanh, N. T. K.: Seasonal and diurnal variations of black carbon
475 and organic carbon aerosols in Bangkok, J Geophys Res-Atmos, 116, Artn D15302 10.1029/2010jd015563, 2011.
476 Squizzato, S., Masiol, M., Brunelli, A., Pistollato, S., Tarabotti, E., Rampazzo, G., and Pavoni, B.: Factors determining the
477 formation of secondary inorganic aerosol: a case study in the Po Valley (Italy), Atmos Chem Phys, 13, 1927-1939,
478 10.5194/acp-13-1927-2013, 2013.
479 Squizzato, S., and Masiol, M.: Application of meteorology-based methods to determine local and external contributions to
480 particulate matter pollution: A case study in Venice (Italy), Atmos Environ, 119, 69-81, 10.1016/j.atmosenv.2015.08.026,
481 2015.
482 Stockwell, W. R., and Calvert, J. G.: The Mechanism of the HO-SO_2 Reaction, Atmos Environ, 17, 2231-2235, Doi
483 10.1016/0004-6981(83)90220-2, 1983.

484 Strader, R., Lurmann, F., and Pandis, S. N.: Evaluation of secondary organic aerosol formation in winter, Atmos Environ, 33,
485 4849-4863, Doi 10.1016/S1352-2310(99)00310-6, 1999.
486 Tan, J. H., Duan, J. C., He, K. B., Ma, Y. L., Duan, F. K., Chen, Y., and Fu, J. M.: Chemical characteristics of $PM_{2.5}$ during a
487 typical haze episode in Guangzhou, J Environ Sci-China, 21, 774-781, 10.1016/S1001-0742(08)62340-2, 2009.
488 Tan, J. H., Duan, J. C., Ma, Y. L., He, K. B., Cheng, Y., Deng, S. X., Huang, Y. L., and Si-Tu, S. P.: Long-term trends of
489 chemical characteristics and sources of fine particle in Foshan City, Pearl River Delta: 2008-2014, Sci Total Environ, 565,
490 519-528, 10.1016/j.scitotenv.2016.05.059, 2016.
491 Tao, J., Zhang, L. M., Engling, G., Zhang, R. J., Yang, Y. H., Cao, J. J., Zhu, C. S., Wang, Q. Y., and Luo, L.: Chemical
492 composition of $PM_{2.5}$ in an urban environment in Chengdu, China: Importance of springtime dust storms and biomass
493 burning, Atmos Res, 122, 270-283, 10.1016/j.atmosres.2012.11.004, 2013.
494 Tao, J., Gao, J., Zhang, L., Zhang, R., Che, H., Zhang, Z., Lin, Z., Jing, J., Cao, J., and Hsu, S. C.: $PM_{2.5}$ pollution in a
495 megacity of southwest China: source apportionment and implication, Atmos Chem Phys, 14, 8679-8699,
496 10.5194/acp-14-8679-2014, 2014.
497 Taus, N., Tarulescu, S., Idomir, M., and Taus, R.: Respiratory exposure to air pollutants, J Environ Prot Ecol, 9, 15-25, 2008.
498 Tian, M., Wang, H. B., Chen, Y., Yang, F. M., Zhang, X. H., Zou, Q., Zhang, R. Q., Ma, Y. L., and He, K. B.: Characteristics
499 of aerosol pollution during heavy haze events in Suzhou, China, Atmos Chem Phys, 16, 7357-7371,
500 10.5194/acp-16-7357-2016, 2016.
501 Tian, Y. Z., Wu, J. H., Shi, G. L., Wu, J. Y., Zhang, Y. F., Zhou, L. D., Zhang, P., and Feng, Y. C.: Long-term variation of the
502 levels, compositions and sources of size-resolved particulate matter in a megacity in China, Sci Total Environ, 463,
503 462-468, 10.1016/j.scitotenv.2013.06.055, 2013.
504 Tie, X. X., and Cao, J. J.: Aerosol pollution in China: Present and future impact on environment, Particuology, 7, 426-431,
505 10.1016/j.partic.2009.09.003, 2009.
506 Turpin, B. J., and Huntzicker, J. J.: Identification of Secondary Organic Aerosol Episodes and Quantitation of Primary and
507 Secondary Organic Aerosol Concentrations during Scaqs, Atmos Environ, 29, 3527-3544, Doi
508 10.1016/1352-2310(94)00276-Q, 1995.
509 Turpin, B. J., and Lim, H. J.: Species contributions to PM2.5 mass concentrations: Revisiting common assumptions for
510 estimating organic mass, Aerosol Sci Tech, 35, 602-610, Doi 10.1080/02786820152051454, 2001.
511 Wang, D. F., Zhou, B., Fu, Q. Y., Zhao, Q. B., Zhang, Q., Chen, J. M., Yang, X., Duan, Y. S., and Li, J.: Intense secondary
512 aerosol formation due to strong atmospheric photochemical reactions in summer: observations at a rural site in eastern
513 Yangtze River Delta of China, Sci Total Environ, 571, 1454-1466, 10.1016/j.scitotenv.2016.06.212, 2016.
514 Wang, H. B., Shi, G. M., Tian, M., Zhang, L. M., Chen, Y., Yang, F. M., and Cao, X. Y.: Aerosol optical properties and
515 chemical composition apportionment in Sichuan Basin, China, Sci Total Environ, 577, 245-257,
516 10.1016/j.scitotenv.2016.10.173, 2017.
517 Wang, H. L., Qiao, L. P., Lou, S. R., Zhou, M., Chen, J. M., Wang, Q., Tao, S. K., Chen, C. H., Huang, H. Y., Li, L., and
518 Huang, C.: $PM_{2.5}$ pollution episode and its contributors from 2011 to 2013 in urban Shanghai, China, Atmos Environ, 123,
519 298-305, 10.1016/j.atmosenv.2015.08.018, 2015.
520 Wongphatarakul, V., Friedlander, S. K., and Pinto, J. P.: A comparative study of $PM_{2.5}$ ambient aerosol chemical databases,
521 Environ Sci Technol, 32, 3926-3934, Doi 10.1021/Es9800582, 1998.
522 Yang, F., Huang, L., Duan, F., Zhang, W., He, K., Ma, Y., Brook, J. R., Tan, J., Zhao, Q., and Cheng, Y.: Carbonaceous
523 species in $PM_{2.5}$ at a pair of rural/urban sites in Beijing, 2005-2008, Atmos Chem Phys, 11, 7893-7903,
524 10.5194/acp-11-7893-2011, 2011a.
525 Yang, F., Tan, J., Zhao, Q., Du, Z., He, K., Ma, Y., Duan, F., Chen, G., and Zhao, Q.: Characteristics of $PM_{2.5}$ speciation in
526 representative megacities and across China, Atmos Chem Phys, 11, 5207-5219, 10.5194/acp-11-5207-2011, 2011b.
527 Yang, Y. R., Liu, X. G., Qu, Y., An, J. L., Jiang, R., Zhang, Y. H., Sun, Y. L., Wu, Z. J., Zhang, F., Xu, W. Q., and Ma, Q. X.:
528 Characteristics and formation mechanism of continuous hazes in China: a case study during the autumn of 2014 in the
529 North China Plain, Atmos Chem Phys, 15, 8165-8178, 10.5194/acp-15-8165-2015, 2015.

Zhang, Q., Quan, J. N., Tie, X. X., Li, X., Liu, Q., Gao, Y., and Zhao, D. L.: Effects of meteorology and secondary particle formation on visibility during heavy haze events in Beijing, China, Sci Total Environ, 502, 578-584, 10.1016/j.scitotenv.2014.09.079, 2015a.

Zhang, Q., Shen, Z. X., Cao, J. J., Zhang, R. J., Zhang, L. M., Huang, R. J., Zheng, C. J., Wang, L. Q., Liu, S. X., Xu, H. M., Zheng, C. L., and Liu, P. P.: Variations in PM2.5, TSP, BC, and trace gases (NO_2, SO_2, and O_3) between haze and non-haze episodes in winter over Xi'an, China, Atmos Environ, 112, 64-71, 10.1016/j.atmosenv.2015.04.033, 2015b.

Zhang, R., Jing, J., Tao, J., Hsu, S. C., Wang, G., Cao, J., Lee, C. S. L., Zhu, L., Chen, Z., Zhao, Y., and Shen, Z.: Chemical characterization and source apportionment of $PM_{2.5}$ in Beijing: seasonal perspective, Atmos Chem Phys, 13, 7053-7074, 10.5194/acp-13-7053-2013, 2013.

Zhang, Y., Huang, W., Cai, T. Q., Fang, D. Q., Wang, Y. Q., Song, J., Hu, M., and Zhang, Y. X.: Concentrations and chemical compositions of fine particles ($PM_{2.5}$) during haze and non-haze days in Beijing, Atmos Res, 174, 62-69, 10.1016/j.atmosres.2016.02.003, 2016.

Zhang, Y. H., Hu, M., Zhong, L. J., Wiedensohler, A., Liu, S. C., Andreae, M. O., Wang, W., and Fan, S. J.: Regional Integrated Experiments on Air Quality over Pearl River Delta 2004 (PRIDE-PRD2004): Overview, Atmos Environ, 42, 6157-6173, 10.1016/j.atmosenv.2008.03.025, 2008.

Zhao, M. F., Huang, Z. S., Qiao, T., Zhang, Y. K., Xiu, G. L., and Yu, J. Z.: Chemical characterization, the transport pathways and potential sources of $PM_{2.5}$ in Shanghai: Seasonal variations, Atmos Res, 158, 66-78, 10.1016/j.atmosres.2015.02.003, 2015.

Zhao, P. S., Dong, F., He, D., Zhao, X. J., Zhang, X. L., Zhang, W. Z., Yao, Q., and Liu, H. Y.: Characteristics of concentrations and chemical compositions for $PM_{2.5}$ in the region of Beijing, Tianjin, and Hebei, China, Atmos Chem Phys, 13, 4631-4644, 10.5194/acp-13-4631-2013, 2013a.

Zhao, X. J., Zhao, P. S., Xu, J., Meng, W., Pu, W. W., Dong, F., He, D., and Shi, Q. F.: Analysis of a winter regional haze event and its formation mechanism in the North China Plain, Atmos Chem Phys, 13, 5685-5696, 10.5194/acp-13-5685-2013, 2013b.

Zheng, B., Zhang, Q., Zhang, Y., He, K. B., Wang, K., Zheng, G. J., Duan, F. K., Ma, Y. L., and Kimoto, T.: Heterogeneous chemistry: a mechanism missing in current models to explain secondary inorganic aerosol formation during the January 2013 haze episode in North China, Atmos Chem Phys, 15, 2031-2049, 10.5194/acp-15-2031-2015, 2015a.

Zheng, G. J., Duan, F. K., Su, H., Ma, Y. L., Cheng, Y., Zheng, B., Zhang, Q., Huang, T., Kimoto, T., Chang, D., Poschl, U., Cheng, Y. F., and He, K. B.: Exploring the severe winter haze in Beijing: the impact of synoptic weather, regional transport and heterogeneous reactions, Atmos Chem Phys, 15, 2969-2983, 10.5194/acp-15-2969-2015, 2015b.

Atmos. Chem. Phys. Discuss., doi:10.5194/acp-2017-258, 2017
Manuscript under review for journal Atmos. Chem. Phys.
Discussion started: 10 April 2017

Atmospheric Chemistry and Physics Discussions

Table 1 Annual and seasonal mean concentrations of $PM_{2.5}$ and major chemical components (μg m^{-3}) at CD and CQ during 2014-2015.

	CD					CQ				
	Autumn	Winter	Spring	Summer	Annual	Autumn	Winter	Spring	Summer	Annual
$PM_{2.5}$	62.1±38.4	113.5±47.8	48.0±25.2	45.1±15.2	67.0±43.4	56.3±23.6	115.1±53.9	58.3±24.6	54.2±16.2	70.9±41.4
SO_4^{2-}	10.5±6.5	16.4±7.1	8.3±5.9	9.7±4.7	11.2±6.8	9.9±4.7	17.5±7.4	10.4±6.5	11.1±5.7	12.2±6.8
NO_3^-	9.3±7.4	17.5±8.8	5.9±3.6	3.9±2.2	9.1±8.0	7.8±3.8	15.8±9.5	5.9±5.0	1.6±1.3	7.7±7.6
NH_4^+	6.9±4.8	12.7±5.4	5.1±3.2	4.2±1.9	7.2±5.2	5.7±2.8	11.3±5.2	5.2±3.0	4.0±2.1	6.6±4.4
Cl^-	1.9±1.2	3.4±1.9	0.6±0.4	0.2±0.2	1.5±1.7	0.8±0.4	1.6±1.2	0.5±0.5	0.04±0.03	0.7±0.9
K^+	0.6±0.4	1.2±0.6	0.6±0.5	0.5±0.2	0.7±0.5	0.5±0.2	1.2±0.7	0.5±0.2	0.3±0.1	0.6±0.5
OC	10.4±6.1	19.7±8.4	6.3±3.7	7.4±1.5	10.9±7.6	9.7±4.7	24.2±13.6	10.0±5.1	8.5±3.4	13.1±10.0
EC	3.0±2.1	6.3±3.0	2.7±2.3	2.5±0.7	3.6±2.7	3.8±1.7	5.9±3.2	4.7 ±3.0	3.7±1.5	4.5±2.6
FS	3.2±1.6	4.5±2.0	4.8±3.0	2.7±1.5	3.8±2.2	5.0±2.8	6.3±3.3	9.1±7.6	6.5±4.0	6.7±5.0

Atmos. Chem. Phys. Discuss., doi:10.5194/acp-2017-258, 2017
Manuscript under review for journal Atmos. Chem. Phys.
Discussion started: 10 April 2017

Atmospheric Chemistry and Physics Discussions

Table 2 Pearson's correlation analysis for daily concentrations of major components in $PM_{2.5}$ between CD and CQ, significant correlation ($p<0.01$) are bold faced.

	SO_4^{2-}	NO_3^-	NH_4^+	Cl^-	K^+	OC	EC	FS
Autumn	**0.78**	**0.72**	**0.75**	0.10	**0.76**	**0.87**	**0.79**	0.08
Winter	**0.63**	0.49	**0.60**	**0.51**	**0.77**	**0.83**	**0.80**	**0.64**
Spring	**0.76**	0.39	**0.59**	0.09	**0.68**	**0.78**	**0.74**	0.29
Summer	0. 49	-0.13	0.40	0.37	0.36	0.43	0.23	-0.02
Annual	**0.72**	**0.71**	**0.76**	**0.67**	**0.79**	**0.80**	**0.72**	0.31

Atmos. Chem. Phys. Discuss., doi:10.5194/acp-2017-258, 2017
Manuscript under review for journal Atmos. Chem. Phys.
Discussion started: 10 April 2017

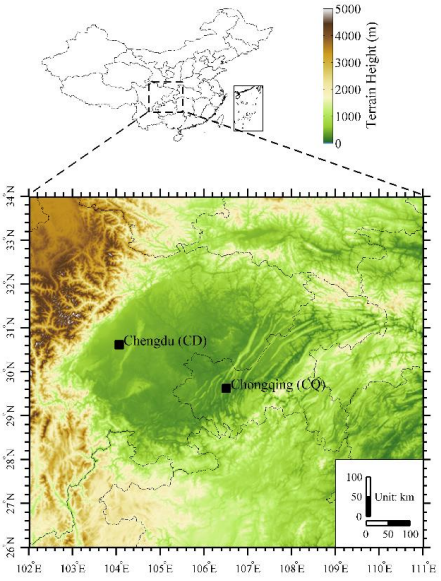

Figure 1. Locations of the sampling sites at Chengdu (CD) and Chongqing (CQ).

Atmos. Chem. Phys. Discuss., doi:10.5194/acp-2017-258, 2017
Manuscript under review for journal Atmos. Chem. Phys.
Discussion started: 10 April 2017

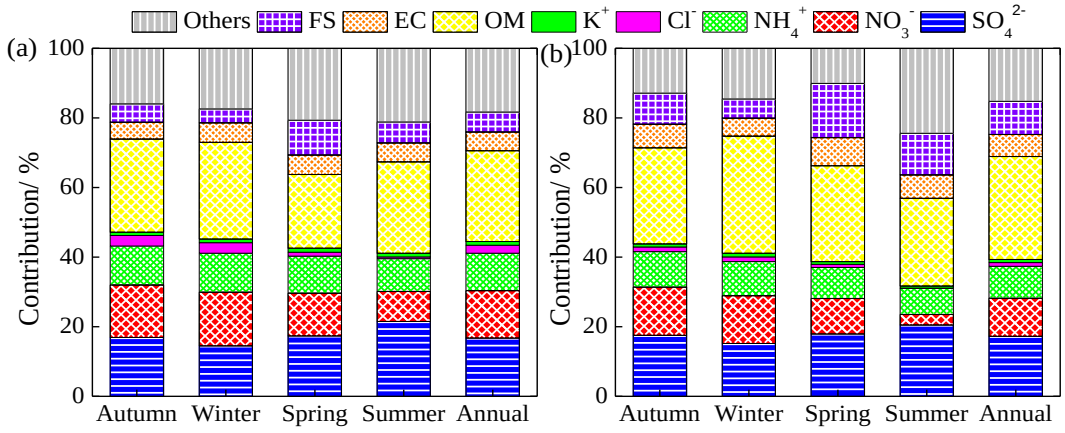

Figure 2. Seasonal and annual contributions of individual chemical components to $PM_{2.5}$ at CD (a) and CQ (b).

Atmos. Chem. Phys. Discuss., doi:10.5194/acp-2017-258, 2017
Manuscript under review for journal Atmos. Chem. Phys.
Discussion started: 10 April 2017

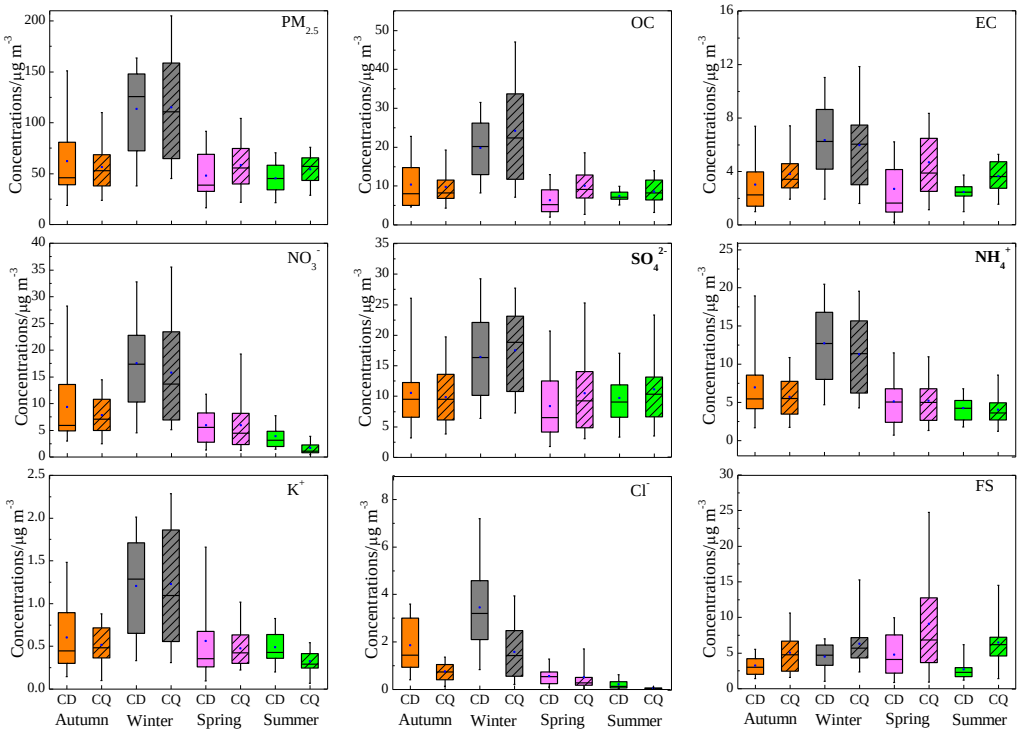

Figure 3. Seasonal variations of major chemical compositions in $PM_{2.5}$. The 5th, 25th, median, 75th, and 95th percentiles are shown in the figure.

Atmos. Chem. Phys. Discuss., doi:10.5194/acp-2017-258, 2017
Manuscript under review for journal Atmos. Chem. Phys.
Discussion started: 10 April 2017

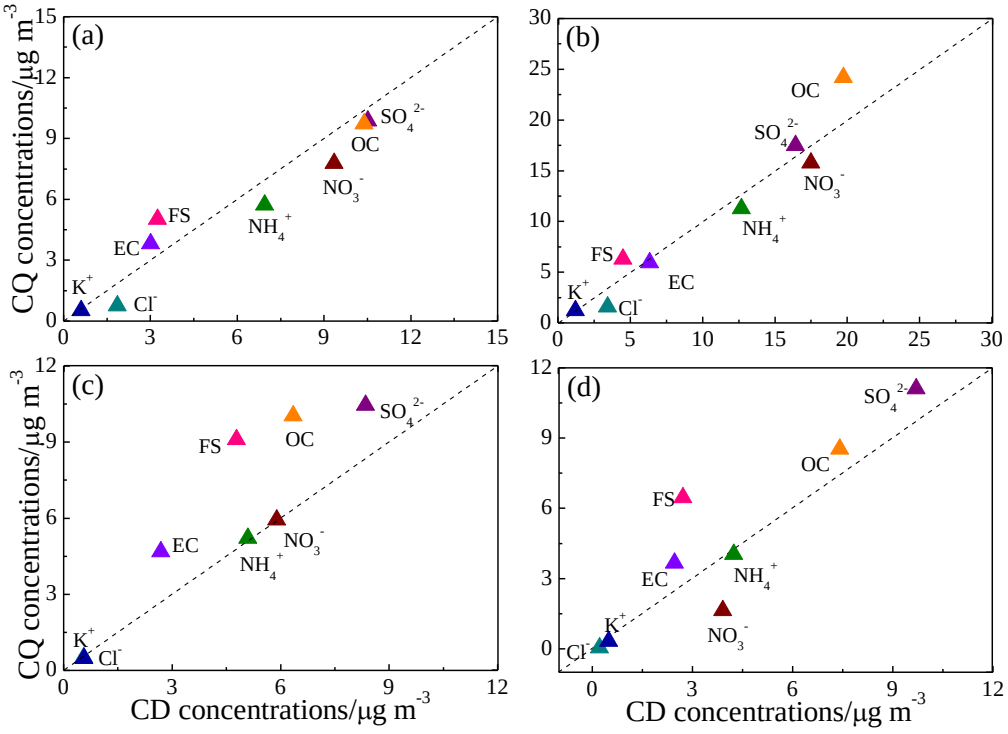

Figure 4. Seasonal mean concentrations of major components in autumn (a), winter (b), spring (c), and summer (d) at CD and CQ sites.

Atmos. Chem. Phys. Discuss., doi:10.5194/acp-2017-258, 2017
Manuscript under review for journal Atmos. Chem. Phys.
Discussion started: 10 April 2017

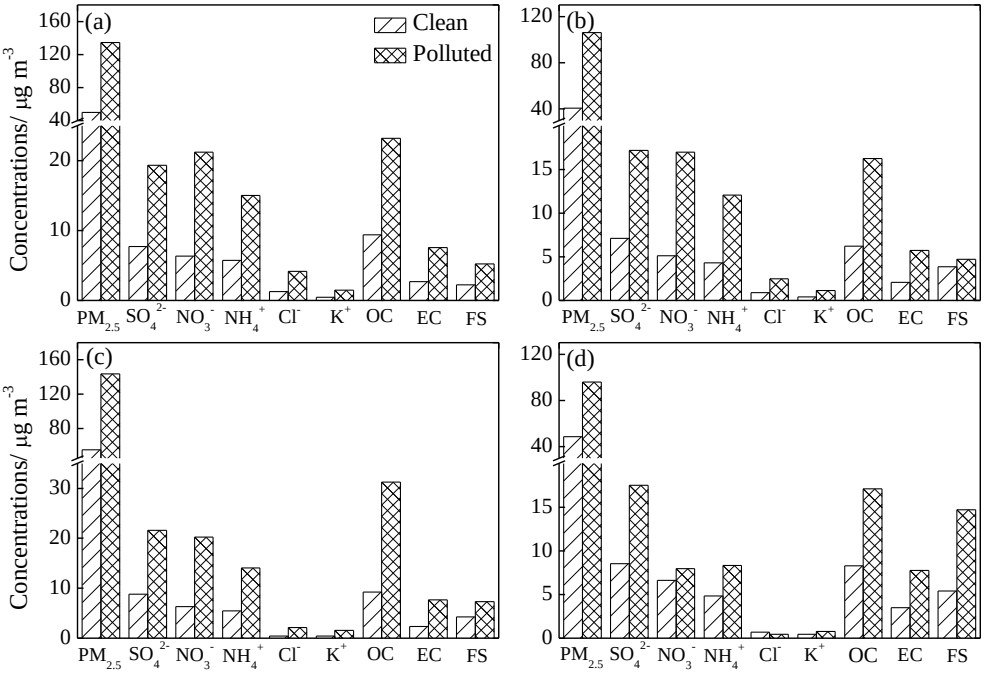

Figure 5. $PM_{2.5}$ and major chemical components on clean and polluted days in the cold (left column) and warm (right column) seasons at CD (upper row) and CQ (lower row).

Atmos. Chem. Phys. Discuss., doi:10.5194/acp-2017-258, 2017
Manuscript under review for journal Atmos. Chem. Phys.
Discussion started: 10 April 2017

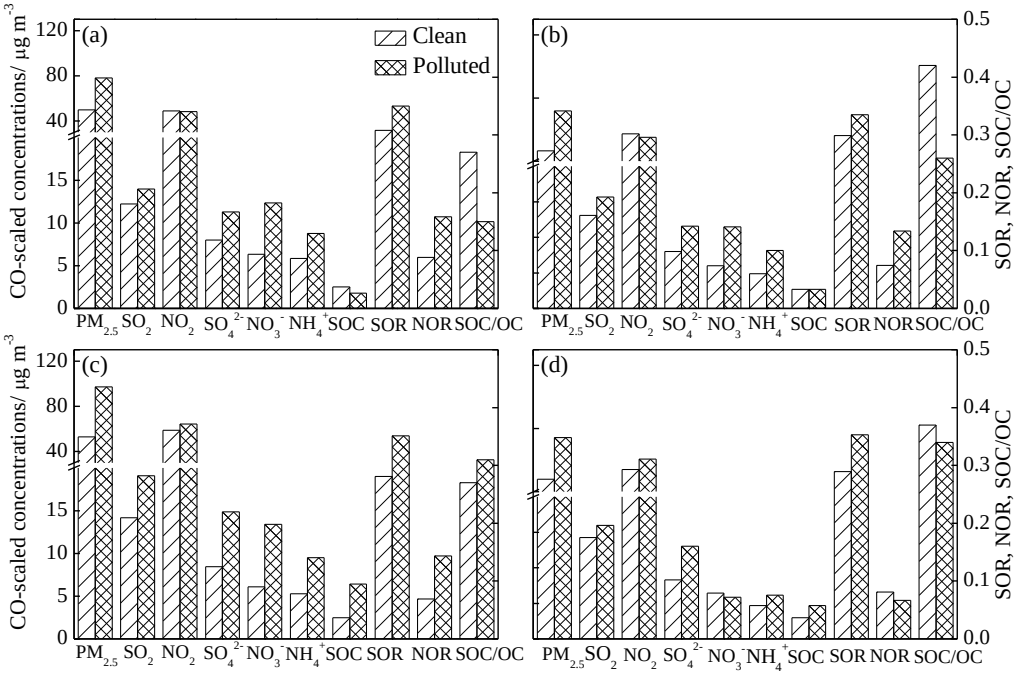

Figure 6. CO-scaled concentrations of various pollutants and the values of SOR, NOR, and SOC/OC in the cold (left column) and warm (right column) seasons at CD (upper row) and CQ (lower row).

Atmos. Chem. Phys. Discuss., doi:10.5194/acp-2017-258, 2017
Manuscript under review for journal Atmos. Chem. Phys.
Discussion started: 10 April 2017

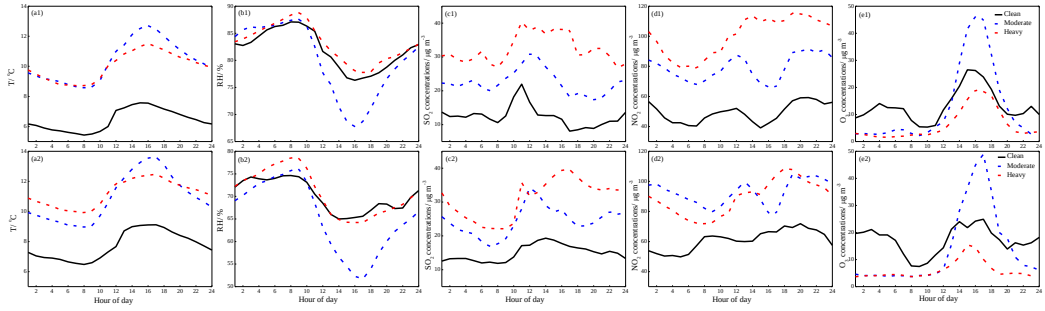

Figure 7. Diurnal variations of T, RH, SO_2, NO_2, and O_3 under different pollution-level conditions in the cold season at CD (upper row) and CQ (lower row). Clean days: $PM_{2.5} \leq 75$ μg m^{-3}; moderate polluted days: $75 < PM_{2.5} \leq 150$ μg m^{-3}; heavy polluted days: $PM_{2.5} > 150$ μg m^{-3}.

Atmos. Chem. Phys. Discuss., doi:10.5194/acp-2017-258, 2017
Manuscript under review for journal Atmos. Chem. Phys.
Discussion started: 10 April 2017

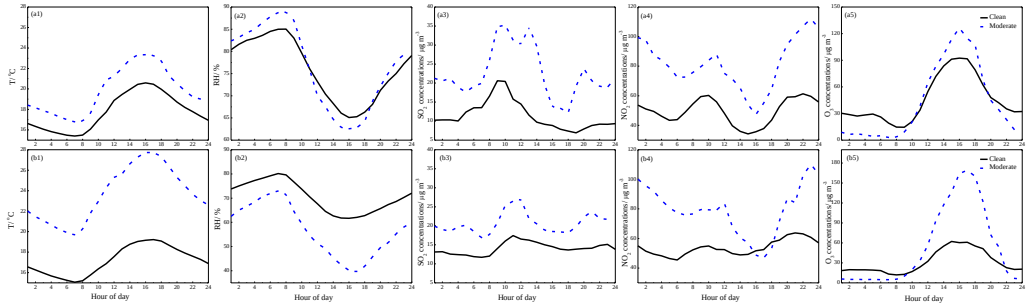

Figure 8. Same as in Figure 7 except in the warm season and only for two pollution-levels.

Atmos. Chem. Phys. Discuss., doi:10.5194/acp-2017-258, 2017
Manuscript under review for journal Atmos. Chem. Phys.
Discussion started: 10 April 2017

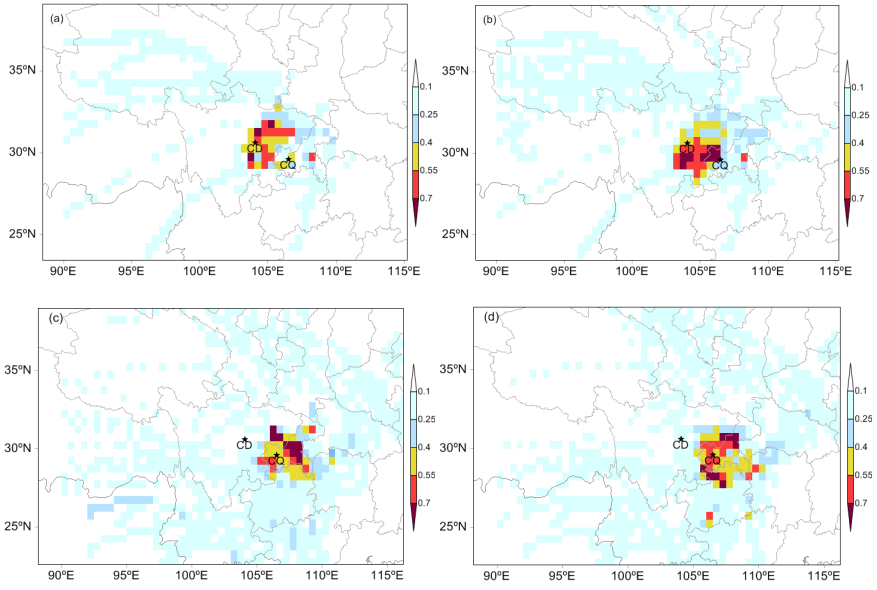

Figure 9. PSCF maps of $PM_{2.5}$ in the cold (left column) and warm (right column) seasons at CD (upper row) and CQ (lower row).